



## MOLECULAR DOCKING STUDY REVEALS PINORESINOL AS A POTENTIAL INHIBITOR FOR NIPAH VIRUS GLYCOPROTEIN

**T. Ekneligoda, O. Perera, H. Mudalige\***

*BMS School of Science, Colombo 6, Sri Lanka*

### INTRODUCTION

Nipah virus (NiV) is a biosafety level 4 (BSL-4) zoonotic pathogen belonging to the *Paramyxoviridae* family and *Henipavirus* genus (Watkinson and Lee, 2016). In 2018, the WHO identified the NiV infection as a blueprint priority disease (WHO, 2018). Among humans, it was first reported in Malaysia in 1998 followed by sporadic outbreaks in Bangladesh and India (Epstein *et al.*, 2006). Natural reservoirs of the NiV are several species of fruit bats belonging to the *Pteropus* genus, which are endemic to South and Southeast Asia (Simons *et al.*, 2014). NiV has a broad secondary host tropism, namely canines, felines, pigs, and hamsters that result in a higher zoonotic potential and pathogenicity towards humans (Ali, Morshed and Hassan, 2015). The primary mode of zoonosis is through contaminated body fluids from the infected species (Epstein *et al.*, 2006). Interhuman transmission occurs through contaminated aerosols, body fluids, and surfaces (Ali *et al.*, 2018). It is a highly trophic virus as its functional cellular attachment receptors in humans are the Ephrin B2 and Ephrin B3 receptors, which are expressed in endothelial cells, smooth muscle cells, and neurons (Sun *et al.*, 2018). Thereby, the associated symptoms among humans are acute febrile encephalitis, and severe pulmonary and cardiac diseases leading to poor disease outcomes (Ropón-Palacios *et al.*, 2019). NiV is an unsegmented, pleomorphic enveloped virus comprising a negatively charged RNA genome (Watkinson and Lee, 2016). Its genome constitutes 6 structural genes that primarily encode 6 functional proteins (Sun *et al.*, 2018). Table 1 represents phytochemicals 1-8 that have shown good binding free energies (BFEs) when docked using the LibDock module of Discovery studio 4.0 and 9-14 that have depicted inhibitory activity on *Paramyxoviridae* family viruses in clinical trials. Phytochemicals were chosen as they can inhibit viral entry, transcription, and translation with minimum side/adverse effects (Ghildiya *et al.*, 2020).

**Table 1:** Phytochemicals utilised in the study.

	Generic Name	Known actions	Sri Lankan Plant Source	Reference
1	Nirphyllin	–	<i>Phyllanthus amarus</i>	Raja <i>et al.</i> , 2020.
2	Niranthin	Anti-inflammatory and antiallodynic actions through its antagonistic action on the PAF receptor binding sites.		
3	Tetrahydrobisdemethoxycurcumin	Reported to reduce the arsenic-induced dyslipidaemia, mitochondrial toxicity, and ultrastructural alterations in rat liver on pre-treatment.	<i>Curcuma longa</i>	
4	Isogingerenone B	Anti-inflammation, antioxidation, superoxide scavenging, and antihepatotoxicity.	<i>Zingiber officinale</i>	
5	Gingerenone A			
6	Gingerenone C			
7	Hexahydrocurcumin	Shows bioactivity than curcumin via in vitro and in vivo, antioxidant, anti-inflammatory, antitumor, and cardiovascular protective properties are depicted.		



8	Salannic acid	Antioxidant, anti-inflammatory, and antipyretic actions.	<i>Azadirachta indica</i>	
9	Pinoresinol	Treat colorectal cancer, hypoglycemic agent, and shows antiviral activity against <i>Paramyxoviridae</i> family.	<i>Euphorbia hirta</i>	Ebenzer <i>et al.</i> , 2019. Li <i>et al.</i> , 2015.
10	Syringaresinol	Depicts anti-inflammatory actions and anti-viral activity against <i>Paramyxoviridae</i> family.		
11	Pinoresinol glucoside	Shows antiviral activity against the <i>Paramyxoviridae</i> family.		
12	Quercetin	Demonstrates antioxidant, anti-inflammatory, and antitumor effects. Side effects are headache, kidney damage, and upset stomach. By-product of quercetin leads to loss of protein function.		
13	Gallic acid	Antimicrobial, anti-obesity, and antioxidant properties.		
14	Epigallocatechin gallate	Antioxidant, anti-inflammatory, anti-stress, reduce heart disease, promote weight loss, and prevents degenerative brain diseases such as Alzheimer's and Parkinson's.	<i>Camellia sinensis</i>	Xu, Xu and Zheng, 2017.

The docking protocol was validated via the redocking technique by using the natural ligand isopropyl alcohol (IPA) of 2VSM followed by the Ramachandran plot analysis of the redocked complex relative to 2VSM's Ramachandran plot (Zheng *et al.*, 2022). Subsequently, the redocked ligand was superimposed to the native co-crystallized ligand and the corresponding RMSD value was obtained (Shivanika *et al.*, 2020). By achieving a root mean square deviation (RMSD) value  $\leq 2.00 \text{ \AA}$  for the best redocked pose, the conformation and orientation of the ligand is validated to be true (Al-Khodairy *et al.*, 2013). Since the result of the redocking was utilised for the superimposition, the above validates all results in the study.

## OBJECTIVE

Despite the sporadic outbreaks and exorbitant fatality rates of ~70%, there are no licenced treatments available against the NiV infection currently. Treatment methods employed during outbreaks include supportive care and treatment of symptoms (Raveendran *et al.*, 2018). Reasons for the lack of specific treatments are sporadic outbreaks with limited distribution, the BSL-4 pathogen, and limited knowledge. Accordingly, it is pivotal to create new treatments to prevent the triggering of an epidemic. Research on developing new treatments such as immunotherapeutic treatment using the antibody - m102.4 (Deka and Morshed, 2018), use of immunoinformatics to create a vaccine (Johnson and Georrge, 2020), repurposing already approved FDA drugs (Rajput *et al.*, 2021), and executing molecular docking studies to discover new lead compounds as therapeutic drugs are underway. This study targeted the prediction of potential phytochemicals that are endemic to South Asia with known antiviral activities that can act against NiV-G using bioinformatic computational protein-ligand docking techniques.

## MATERIALS AND METHODOLOGY

Docking protocols follow computational pathways based on search algorithms and scoring functions (Li, Fu and Zhang, 2019 and Dias and de Azevedo, 2008). Docking is achieved by following the lowest energy pathways, mimicking the natural course by considering intermolecular interactions such as hydrophobic, hydrogen bonds, and electrostatic forces (Ballante, 2018 and Hernández-Santoyo *et al.*, 2013). The overall interaction energies provide the binding free energy of the docked complex, which is utilised to predict the best fit ligand



(Wagner *et al.*, 2019). Blind docking (BD) is done without any prior knowledge on the active site of the protein (Zhang *et al.*, 2020). For this study, the blind docking technique was employed as the literature available on computational research to explicitly verify the active site of NiV-G is scarce. Thereby, through this study, further molecular docking simulation studies can be carried out to further verify the active site coordinates of the NiV-G. AutoDock 4.2.6 (AD4) (Morris, Huey and Olson 2008) utilises a combination of the Empirical Force Field and Lamarckian Genetic algorithm, limiting the flexibility of the protein and expediting the binding conformations and free energy associations of the docked complex (Morris *et al.*, 2009). Chimera (Butt *et al.*, 2020) is a high-quality performance software with a core and extensions that support docking, visualisation, and analysis for users. PyMOL (Seeliger and de Groot, 2010), LIGPLOT (Wallace, Laskowski and Thornton, 1995), and BIOVIA Discovery Studio Visualiser (BIOVIA, Dassault Systèmes, 2021) are employed to visualise and analyse the docked complexes and associated data.

For this study, the Nipah virus attachment glycoprotein (NiV-G) was chosen as the protein receptor (Bowden *et al.*, 2008). NiV-G is a virulent factor that mediates the adhesion of the NiV to the host cell and pathogenicity (Guillaume *et al.*, 2020). RCSB PDB accommodates four structures of the NiV-G from which PDB ID: 2VSM was selected as it had the lowest x-ray diffraction resolution of 1.80 Å and the highest score of 86.1% for the most favoured regions in the Ramachandran plot (Bowden *et al.*, 2008 and Laskowski *et al.*, 1993). 2VSM comprises chains A and B from which chain A was utilised for docking. Chain B is the human cell surface receptor and Ephrin-B2, which complexes with the NiV-G (chain A) during host cell attachment (Xu, Broder and Nikolov, 2012). To prevent the attachment of the NiV to the host cell and downstream pathogenicity, chain A should be biologically inhibited. Phytochemicals that depicted potential inhibitory effects on NiV-G were selected.

**Table 2:** Materials utilised for the study.

Hardware	Software	Webtools	Other	Phytochemicals
Computer with an intel core i7-7500U containing a 16.0GB RAM, 64-bit operating system and the Windows 10 application system	Python 3.10 ( <a href="https://www.python.org/">https://www.python.org/</a> )	NCBI PubChem ( <a href="https://pubchem.ncbi.nlm.nih.gov/">https://pubchem.ncbi.nlm.nih.gov/</a> )	Network connection 2.4 GHz and 72/72 (Mbps)	Syringaresinol
	MGLTools 1.5.6 ( <a href="https://ccsb.scripps.edu/mgltools/">https://ccsb.scripps.edu/mgltools/</a> )	RCSB PDB ( <a href="https://www.rcsb.org/">https://www.rcsb.org/</a> )		Gingerenone A
	AutoDock 4.2.6 ( <a href="https://autodock.scripps.edu/">https://autodock.scripps.edu/</a> )	ZINC ( <a href="https://zinc.dockinc.org/">https://zinc.dockinc.org/</a> )		Gingerenone C
	PyMOL 2.5 ( <a href="https://pymol.org/2/">https://pymol.org/2/</a> )	SwissADME ( <a href="http://www.swissadme.ch/">http://www.swissadme.ch/</a> )		Salannic acid
	Java Oracle ( <a href="https://www.java.com/en/">https://www.java.com/en/</a> )	PROCHECK v 3.5 ( <a href="http://www.csb.yale.edu/userguides/datanip/procheck/manual/index.html">http://www.csb.yale.edu/userguides/datanip/procheck/manual/index.html</a> )		Pinoresinol
	LIGPLOT+ v 2.2 ( <a href="https://www.ebi.ac.uk/thornton-srv/software/LigPlus/">https://www.ebi.ac.uk/thornton-srv/software/LigPlus/</a> )			Tetrahydrobisdemethoxycurcumin



	UCSF Chimera 1.15 ( <a href="https://www.cgl.ucsf.edu/chimera/">https://www.cgl.ucsf.edu/chimera/</a> )			Nirphyllin
	BIOVIA Discovery Studio Visualiser ( <a href="https://discover.3ds.com/discovery-studio-visualizer-download">https://discover.3ds.com/discovery-studio-visualizer-download</a> )			Niranthin
	Open Babel 2.4.1 ( <a href="https://sourceforge.net/projects/openbabel/">https://sourceforge.net/projects/openbabel/</a> )			Quercetin
				Gallic acid
				Hexahydrocurcumin
				Isogingerenone B

### Receptor and ligand preparation

Preparation of the receptor and ligands were done by following the AD4 tool manual. Preparation of 2VSM for docking was done in AD4. The 3D structure was retrieved from RCSB PDB in *.pdb* format and loaded onto AD4. The water molecules, chain B and heteroatoms (IPA and 2-acetamido-2-deoxy-beta-D-glucopyranose/ NAG) were removed followed by the addition of polar hydrogen atoms and merging of non-polar hydrogen atoms (Pathania, Randhawa and Kumar, 2019). Subsequently, 3.048 Kollman charges were added and AD4 type atoms were assigned and saved in *.pdbqt* format.

Preparation of the ligands for docking was performed in AD4. The 3D structures of the ligands were retrieved from PubChem/ZINC databases in *.sdf* format and converted to *.pdb* format using Open Babel. Thereafter, they were loaded on to AD4 separately with correspondence to each run. Preparation was done by setting the TORSDOF, merging non-polar hydrogen atoms, adding Marsili-Gasteiger partial charges, and being saved in the *.pdbqt* format (Morris, Huey and Olson, 2008).

The grid box was generated using AD4 to provide the area of ligand binding for the AD4 program. The receptor was enclosed in whole for BD. The X, Y, and Z dimensions were 120×126×114 and the spacing was 0.500 Å. Subsequently, in AD4 the number of Genetic algorithm runs (iterations) and population size were set to 50 and 300, respectively (Morris *et al.*, 2014), which was followed by the execution of AutoGrid and AutoDock programs. The *.dlg* file generated following the docking was utilised to identify the best BFE, inhibitory constant (Ki), and conformation of each ligand/docked complex. Prior to visualisation, the best docked conformation of each ligand was written into a *.pdbqt* file utilising AD4 and converted to a *.pdb* (Docked.*pdb*) file using Open Babel. Subsequently, the Docked.*pdb* file was loaded on to PyMOL and Chimera separately, followed by the adjustment of parameters to visualise each docked complex in publication mode (Butt *et al.*, 2020 and Seeliger and de Groot, 2010). The Docked.*pdb* file was loaded on to BIOVIA, and the parameters were altered to acquire the 3D ligand interactions for amino acid interactions (AAI) analysis, and the 3D ligand interactions in the 2D plane were acquired for the analysis of hydrogen interactions (HI) and hydrophobic interactions (HPI) (BIOVIA, Dassault Systèmes, 2021), whereas by loading the Docked.*pdb* onto LIGPLOT, the AAI and HI were analysed in 2D (Laskowski and Swindells, 2011).

The absorption, distribution, metabolism, and excretion (ADME) properties of the phytochemicals were analysed to assess their druggability using SwissADME (Kalbhor *et al.*, 2021). The druggability was evaluated primarily based on the Lipinski's rule of five (Benet *et*



al., 2016). Here, the SMILES ID of each phytochemical was uploaded, and the properties generated by the webtool were utilised for analysis.

### Validation

IPA was redocked on to 2VSM and the best BFE was analysed (by using the procedure followed in the study). The .pdb structure of the redocked complex was uploaded to PROCHECK and the generated Ramachandran plot (Laskowski *et al.*, 1993) was analysed in comparison to the Ramachandran plot of 2VSM. Subsequently, the redocked IPA was superimposed to the native co-crystallised structure acquired from RCSB PDB using PyMOL and the superimposed structures were visualised, and the corresponding RMSD value generated via PyMOL was analysed (Berry, Fielding and Gamielien, 2015).

### RESULTS

**Table 3:** BFE, Ki acquired from AD4 and HI, and HPI acquired from BIOVIA of the phytochemicals.

Ligand	BFE (kcal/mol)	Ki (nM)	Interactions			
			HI		HPI	
			No.	Residue	No.	Residue
Pinoresinol	-8.65	455.44	6	Asp461, Lys376, Tyr377, Asn378, Asn381, Asp433	6	Leu436, Pro383, Pro383, Arg435, Arg435, Trp460
Salannic acid	-8.36	740.75	4	Pro403, Arg402, Arg402, Leu305	3	Ile401, Trp504, Leu305
Syringaresinol	-8.06	1240	5	Asp225, Gly355, Gly355, Asp446, Leu567	6	Ile356, Lys357, Leu567, Val255, Phe566, Phe566
Gingerenone C	-7.92	1550	4	Ile514, Asn564, Gly355, Asp446	4	Leu448, Ile572, Cys565, Ile356
Gingerenone A	-7.75	2100	3	Asp433, Arg435, Tyr377	6	Trp460, Leu436, Arg435, Pro383, Pro383, Lys386
Quercetin	-7.59	2750	6	Tyr377, Arg435, Gln434, Leu436, Lys376, Asn381	2	Arg435, Leu436
Niranthin	-7.34	4150	5	Gly227, Glu226, Asn564, Asp446, Ser447	9	Phe512, Tyr445, Ile356, Met224, Val255, Val255, Phe566, Phe566, Phe566
Tetrahydrobisdemethoxycurcumin	-7.28	4590	3	Val255, Gly355, Asp446	2	Val255, Phe566
Isogingerenone B	-7.23	5000	3	Leu513, Leu567, Val255	8	Phe512, Ile572, Ile514, Cys565, Cys565, Phe566, Phe566, Phe566, Val255
Nirphyllin	-7.02	7140	2	Asn564, Cys565	4	Phe566, Phe566, Met224, Met224
Hexahydrocurcumin	-6.87	9200	4	Leu567, Tyr228, Met224, Leu513	8	Phe566, Val255, Met244, Met244, Ile572, Leu448, Leu448, Leu567
Gallic acid	-6.12	32550	4	Lys199, Lys596, Lys596, Lys596	2	Lys199, Lys596

### Visualisation of the best docked pose, HI, and HPI of Pinoresinol

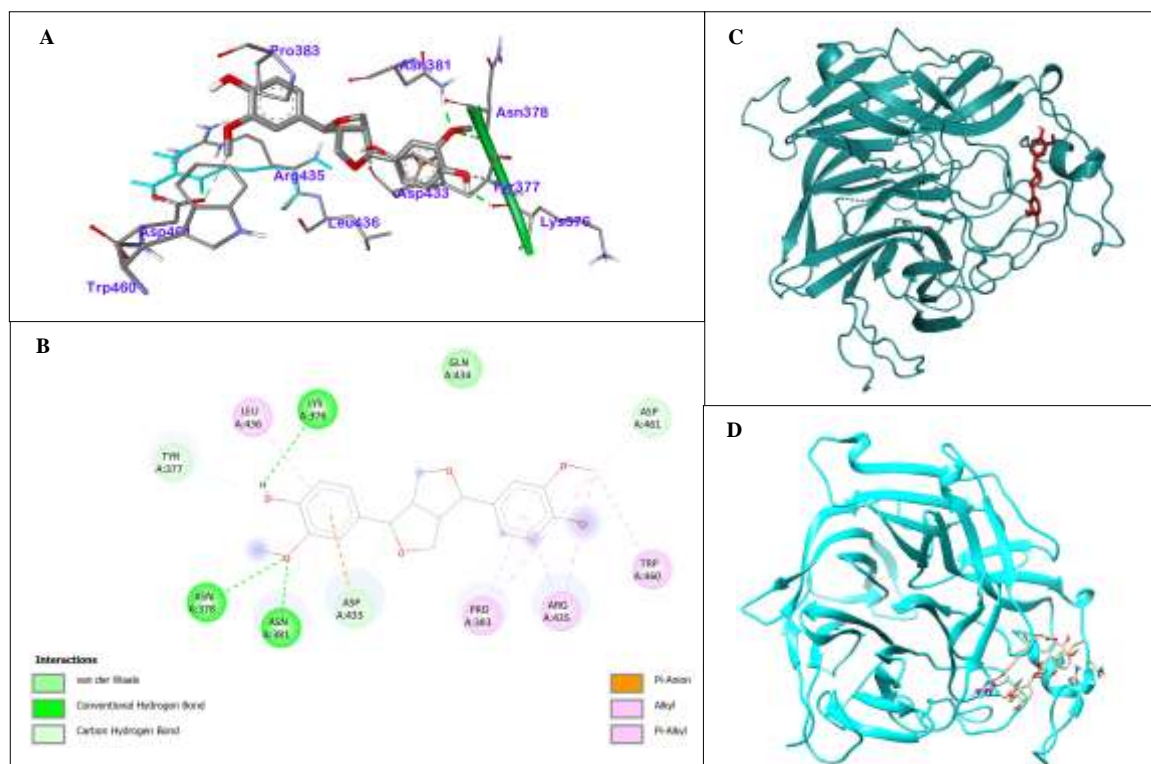


**Figure 1:** A- 3D pinoresinol (ligand) AAI interactions with 2VSM acquired from BIOVIA. B- 2D pinoresinol (ligand) HI (green) and HPI (pink) interactions with 2VSM acquired from BIOVIA. C- 2VSM (teal blue)/pinoresinol (firebrick red) docked pose visualised using PyMOL. D- 2VSM (light blue)/pinoresinol (gold) docked pose visualised using Chimera.

**Table 4:** ADME properties of the phytochemicals acquired from SwissADME.

Phytochemical	*MW (g/mol)	NHA	SC	GI	BBB	vROF	BS	Consensus LogP <sub>o/w</sub>
Nirphyllin	448.51	32	moderately soluble	high	×	?	0.55	3.51
Niranthin	432.51	31	Moderately soluble	high	?	?	0.55	3.89
Tetrahydrobisdemethoxycurcumin	312.36	23	soluble	high	?	?	0.55	2.91
Isogingerenone B	386.44	28	moderately soluble	high	×	?	0.55	3.63
Gingerenone A	356.41	26	moderately soluble	high	?	?	0.55	3.65
Gingerenone C	326.39	24	moderately soluble	high	?	?	0.55	3.60
Hexahydrocurcumin	374.43	27	soluble	high	×	?	0.55	2.92
Salannic acid	458.44	33	soluble	high	×	?	0.56	2.19
Pinoresinol	358.39	26	soluble	high	?	?	0.55	2.26
Syringaresinol	418.44	30	soluble	high	×	?	0.55	2.33
Gallic acid	170.12	12	very soluble	high	×	?	0.56	0.21
Quercetin	302.24	22	soluble	high	×	?	0.55	1.23

\*MW: molecular weight (Reference range/RR: <500g/mol), NHA: no. of heavy atoms, SC: solubility class, GI: gastrointestinal absorption, BBB: blood brain barrier permeation, vROF: Lipinski's rule of five acceptance, BS: bioavailability score (RR: 0.4-0.6), Consensus LogP<sub>o/w</sub>: lipophilicity (RR: ≤5.0) (Daina, Michielin and Zoete, 2017).





## Validation

The redocking of IPA portrayed a BFE of -3.65 kcal/mol and Asn509 and Ile464 were observed to be making AAI with IPA in the redocked and native 2VSM structures, thereby validating the docking protocol utilised. 2VSM depicted a Ramachandran score of 86.1% with 408 out of 474 amino acid residues in the favourable regions whereas the redocked complex showed a Ramachandran score of 85.5% with 306 out of 358 amino acid residues in the favourable region. The Ramachandran score reduction was due to the removal of chain B for docking (Laskowski *et al.*, 1993). The orientation and conformation of the best redocked pose was validated via the generation of a RMSD value of 1.562 Å (Al-Khodairy *et al.*, 2013).

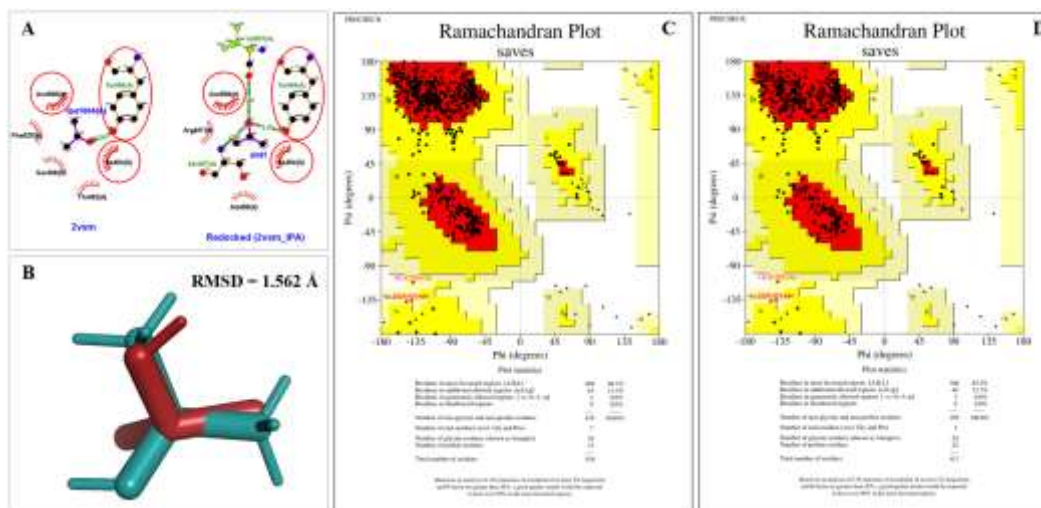


**Figure 2:** A – 2D LIGPLOT ligand interactions of the native 2VSM structure (left) and redocked complex (right) depicting common AAI. B – Superimposed ligand structure of the native IPA (blue) and redocked IPA (red) with a RMSD of 1.562Å. In the Ramachandran plots, the most favourable regions are depicted in red, and the amino acids are black squared dots. C - Ramachandran plot of 2VSM. D – Ramachandran plot of the redocked complex.

## DISCUSSION

During the preparation of 2VSM, water molecules were deleted to expose the binding surfaces to the ligand. Generally, water molecules are not involved in binding and therefore, is removed to reduce the scope of computational hassle and prevent the formation of undesirable H-bonds during binding (Huang and Shoichet, 2008). Heteroatoms were removed to expose the binding surfaces to the ligand as these heteroatoms are frequently computationally added to stabilise the protein in means of thermodynamic principles (Tripathi and Bankaitis, 2017). Thereafter, via the empirical scoring function of AD4, polar hydrogen atoms were added to the structure to optimise the binding affinity and the probability of the H-bond formation, which was followed by the merging of non-polar hydrogen atoms where hydrogens bound to carbons were ‘merged’ by distributing its charge to the adjacent carbon and ‘removing’ the hydrogen to optimise the protein structure by reducing the probability of undesirable H-bond formation (Lippert and Rarey, 2009). AD4 type atoms were assigned to the structure to define the hydrogen bond acceptors/donors and aliphatic/aromatic carbon atoms (Morris *et al.*, 2014). By employing the Lamarckian-Genetic algorithm in AD4, non-polar hydrogen atoms were merged in each ligand to optimise its structure and reduce the probability of undesirable bond formation (Huang and Shoichet, 2008). The TORSDOF was set to define the number of rotatable bonds assigned and the torsion tree was built to allow the ligand to have different conformations when binding to the protein (Morris *et al.*, 2014). Docking in AD4 is an iterative process where the population size (collection of individuals/points in space) and the number of GA runs (number of iterations) define the



quality and reliability of the BFE of each output (Ördög and Grolmusz, 2008). In this study, the optimum population size of 300 and number of GA runs at 50 were utilised.

Primarily, the BFE, which is the sum of final intermolecular energy, Vander Wal forces, HI, desolvation energy, final internal energy, and torsional free energy (Heinzelmann and Gilson, 2021), was employed in the selection of the best performing ligands against 2VSM, along with the ADME properties of the phytochemicals. Here, the principal limitation is the inability of the scoring function to tabulate accurate BFEs as halogen and guanidine-arginine interactions are not considered even though they show significances in regulating the protein-ligand interactions (Yang *et al.*, 2015 and Ren *et al.*, 2014). Furthermore, common AAI corresponding to HI and HPI were identified, and newer interactions were recorded for future analysis. The number of HI are decided from the structure of the ligand and therefore, ligand specificity to the protein is measured using HI, whereas HPI are defined by the binding site residues and thereby, an increased number portrays efficient binding of the ligand to the protein (de Freitas and Schapira, 2017). Accordingly, Arg435, Leu567, Phe566, Leu448, and Cys565 were the most common AAI for both HI and HPI in AD4. Phytochemicals, namely Niranthin, Tetrahydrobisdemethoxycurcumin, Pinoresinol, Gingerenone A, and Gingerenone C demonstrated BBB permeance, which is an effective pharmacokinetic property for treating febrile encephalitis (Ali *et al.*, 2018) that is associated with the NiV infection. The presence of common AAI between the redocked complex and native 2VSM concludes a well performed redock and validation of the docking protocols. The orientation and conformation of the best redocked pose was validated as the RMSD values obtained following superimposition were  $<2.00 \text{ \AA}$ . Here, the principle is that if the orientation acquired from docking can be mimicked by the native structure that will be represented by an RMSD value  $\leq 2.00 \text{ \AA}$  following superimposing, the orientation obtained is allowed. Therefore, the orientations and conformations of ligands generated in this study were validated.

## CONCLUSION AND FUTUREWORK

In conclusion, via considering the BFE and ADME properties, Pinoresinol is the most suitable ligand for a potential drug molecule against the NiV-G. Further, in vivo and in vitro testing can be carried out for verification. Common AAI; Arg435, Leu567, Phe566, Leu448, and Cys565 were identified as novel binding site residues of 2VSM. Molecular dynamics (MD) simulations, which analyse the movements of molecules and atoms within a given span of time using the Newtonian laws of motion and validating the results through the RMSD and RMSF values should be carried out (Car *et al.*, 2005). The off-target interactions of each component can be studied using protein-protein interaction network functional enrichment analysis (Nadeau, Byvsheva and Lavallée-Adam, 2021). Pinoresinol and Syringaresinol from *Euphorbia hirta* can be extracted using the crude aqueous method followed by supercritical fluid chromatography, which can be utilised as leads for antivirals against NiV (Attah *et al.*, 2013 and Gyuris *et al.*, 2009) and the generated Ki values can be employed as references in trials. Moreover, to discover universal therapeutic drugs against the NiV, molecular docking and dynamic studies should be conducted using this study's samples via utilising other NiV receptors.

## REFERENCES

Ali, M. H., Anwar, S., Roy, P. K. and Ashrafuzzaman, M. (2018). 'Virtual Screening for Identification of Small Lead Compound Inhibitors of Nipah Virus Attachment Glycoprotein', *Journal of Pharmacogenomics and Pharmacoproteomics*, 9 (2), pp. 180-188. [Online]. DOI: <http://dx.doi.org/10.4172/2153-0645.1000180> (Accessed: 20 October 2021).





Ali, M. T., Morshed, M. M. and Hassan, F. (2015). 'A Computational Approach for Designing a Universal Epitope-Based Peptide Vaccine Against Nipah Virus', *Interdisciplinary Sciences: Computational Life Sciences*, 7, pp. 177-185. *Springer Link* [Online]. DOI: <https://doi.org/10.1007/s12539-015-0023-0> (Accessed: 7 October 2021).

Al-Khodairy, F. M., Khan, M. K. A., Kunhi, M., Pulicat, M. S., Akhtar, S. and Arif, J. M. (2013). 'In Silico Prediction of Mechanism of Erysolin-induced Apoptosis in Human Breast Cancer Cell Lines', *American Journal of Bioinformatics Research*, 3 (3), pp. 62-71. *ResearchGate* [Online]. Available at: <https://citeseerx.ist.psu.edu/viewdoc/download?doi=10.1.1.1060.9122&rep=rep1&type=pdf> (Accessed: 20 April 2022).

Attah, S. K., Ayeh-Kumi, P. F., Sittie, A., Oppong, I. V. and Nyarko, A. K. (2013). 'Extracts of *Euphorbia hirta* Linn. (*Euphorbiaceae*) and *Rauvolfia vomitoria* Afzel (*Apocynaceae*) Demonstrate Activities Against *Onchocerca volvulus* Microfilariae In Vitro', *BMC Complement Alternate Medicine*, 13 (66). *National Center for Biotechnology Information* [Online]. DOI: <https://dx.doi.org/10.1186%2F1472-6882-13-66> (Accessed: 15 March 2022).

Ballante, F. (2018). 'Protein-Ligand Docking in Drug Design: Performance Assessment and Binding-Pose Selection', *Methods of Molecular Biology*, 1824, pp. 67-88. *PubMed* [Online]. DOI: [https://doi.org/10.1007/978-1-4939-8630-9\\_5](https://doi.org/10.1007/978-1-4939-8630-9_5) (Accessed: 14 November 2021).

Benet, L. Z., Hosey, C. M., Ursu, O. and Oprea, T. I. (2016). 'BDDCS, the Rule of 5 and Drugability', *Advanced Drug Delivery Revisions*, 101, pp. 89-98. *PubMed* [Online]. DOI: <https://doi.org/10.1016%2Fj.addr.2016.05.007> (Accessed: 30 July 2022).

Berry, M., Fielding, B. C. and Gamielidien, J. (2015). 'Potential Broad-Spectrum Inhibitors of the Coronavirus 3CL<sup>pro</sup>: A Virtual Screening and Structure-Based Drug Design Study', *Bioinformatics and Computational Biology of Viruses*, 7 (12), pp. 6642-6660. *Molecular Diversity Preservation International* [Online]. DOI: <https://doi.org/10.3390/v7122963> (Accessed: 20 April 2022).

BIOVIA, Dassault Systèmes. (2021). 'BIOVIA Discovery Studio Visualiser: 2021', *San Diego: Dassault Systèmes*. Available from: <https://3ds.com/products-services/biovia/products> (Accessed: 20 April 2022).

Bowden, T. A., Aricescu, A. R., Gilbert, R. J. C., Grimes, J. M., Jones, E. Y. and Stuart, D. I. (2008). 'Structural basis of Nipah and Hendra virus attachment to their Cell-surface Receptor Ephrin-B2', *Nature, Structural and Molecular Biology*, 6 (15), pp. 567-571. *Nature* [Online]. DOI: <http://www.nature.com/doi/10.1038/nsmb.1435> (Accessed: 14 October 2021).

Butt, S. S., Badshah, Y., Shabbir, M. and Rafiq, M. (2020). 'Molecular Docking Using Chimera and Autodock Vina Software for Nonbioinformaticians', *Journal of Medical Internet Research Bioinformatics Biotechnology*, 1 (1). *Journal of Medical Internet Publications* [Online]. DOI: <https://doi.org/10.2196/14232> (Accessed: 9 October 2021).

Car, R., de Angelis, F., Giannozzi, P. and Marzari, N. (2005). 'First-Principles Molecular Dynamics', *Handbook of Materials Modelling*. *Springer Link* [Online]. DOI: [https://doi.org/10.1007/978-1-4020-3286-8\\_5](https://doi.org/10.1007/978-1-4020-3286-8_5) (Accessed: 20 February 2022).

Daina, A., Michielin, O. and Zoete, V. (2017). 'SwissADME: A Free Web Tool to Evaluate Pharmacokinetics, Drug-likeness and Medicinal Chemistry Friendliness of Small Molecules',



*Scientific Reports*, 7, 42717. *Nature* [Online]. DOI: <https://doi.org/10.1038/srep42717> (Accessed: 20 April 2022).

de Freitas, R. F. and Schapira, M. (2017). ‘A Systematic Analysis of Atomic Protein–Ligand Interactions in the PDB’, *MedChemComm*, 8 (10), pp. 1970-1981. *National Center for Biotechnology Information* [Online]. DOI: <https://dx.doi.org/10.1039%2Fc7md00381a> (Accessed: 15 March 2022).

Deka, M. A. and Morshed, N. (2018). ‘Mapping Disease Transmission Risk of Nipah Virus in South and Southeast Asia’, *Tropical Medicine and Infectious Diseases*, 3 (2), pp. 57. *PubMed* [Online]. DOI: <https://doi.org/10.3390/tropicalmed3020057> (Accessed: 8 Nov 2021).

Dias, R. and de Azevedo, W. F. (2008). ‘Molecular Docking Algorithms’, *Current Drug Targets*, 9 (12), pp. 1040-1047. *Bentham Science* [Online]. DOI: <https://doi.org/10.2174/138945008786949432> (Accessed: 3 December 2021).

Epstein, J. H., Field, H. E., Luby, S., Pulliam, J. R. C. and Daszak, P. (2006). ‘Nipah Virus: Impact, Origins, and Causes of Emergence’, *Current Infectious Disease Reports*, 8, pp. 59-65. *Springer Link* [Online]. DOI: <https://doi.org/10.1007/s11908-006-0036-2> (Accessed: 4 November 2021).

Guillaume, V., Aslan, H., Ainouze, M., Guerbois, M., Wild, T. F., Buckland, R. and Langedijk, K. P. M. (2020). ‘Evidence of a Potential Receptor-Binding Site on the Nipah Virus G Protein (NiV-G): Identification of Globular Head Residues with a Role in Fusion Promotion and Their Localization on an NiV-G Structural Model’, *Journal of Virology*, 80 (15), pp. 7546-7554. *PubMed* [Online]. DOI: <https://doi.org/10.1128/JVI.00190-06> (Accessed: 5 November 2021).

Gyuris, A., Szlávik, L., Minárovits, J., Vasas, A., Molnár, J. and Hohmann, J. (2009). ‘Antiviral Activities of Extracts of *Euphorbia hirta* L. Against HIV-1, HIV-2 and SIVmac251’ *In Vivo (Athens, Greece)*, 23 (3), pp. 429-432. *PubMed* [Online]. PMID: 19454510 (Accessed: 15 March 2022).

Heinzelmann, G. and Gilson, M. K. (2021). ‘Automation of Absolute Protein-Ligand Binding Free Energy Calculations for Docking Refinement and Compound Evaluation’, *Scientific Reports*, 11, 1116. *Scientific Reports* [Online]. DOI: <https://doi.org/10.1038/s41598-020-80769-1> (Accessed: 15 March 2022).

Hernández-Santoyo, A., Tenorio-Barajas, A. Y., Altuzar, V. Vivanco-Cid, H. and Mendoza-Barrera, C. (2013). ‘Protein-Protein and Protein-Ligand Docking’, *Protein Engineering – Technology and Application. IntechOpen* [Online]. DOI: <http://dx.doi.org/10.5772/56376> (Accessed: 11 November 2021).

Huang, N. and Shoichet, B. K. (2008). ‘Exploiting Ordered Waters in Molecular Docking’, *Journal of Medicinal Chemistry*, 51 (16), pp. 4862-4865. *National Center for Biotechnology Information* [Online]. DOI: <https://dx.doi.org/10.1021%2Fjm8006239> (Accessed: 15 March 2022).

Johnson, A. and George, J. J. (2020). ‘Epitope Based Immuno-Informatics Approach for Vaccine Predictions in Nipah Proteins’, *Recent Trends in Science and Technology*, 20 (12). *Figshare* [Online]. DOI: <https://doi.org/10.6084/m9.figshare.13491261> (Accessed: 7 November 2021).



Kalbhor, M. S., Bhowmick, S., Alanazi, A. M., Patil, P. C., and Islam, M. A. (2021). ‘Multi-step Molecular Docking and Dynamics Simulation-based Screening of Large Antiviral Specific Chemical Libraries for Identification of Nipah Virus Glycoprotein Inhibitors’, *Biophysical Chemistry*, 270, 106537. *ScienceDirect* [Online]. DOI: <https://doi.org/10.1016/j.bpc.2020.106537> (Accessed: 20 April 2022).

Laskowski, R. A., MacArthur, M. W., Moss, D. S. and Thornton, J. M. (1993). ‘PROCHECK: A Program to Check the Stereochemical Quality of Protein Structures’, *Journal of Applied Crystallography*, 26 (2), pp. 283-291. *Wiley Online Library* [Online]. DOI: <https://doi.org/10.1107/S0021889892009944> (Accessed: 20 April 2022).

Laskowski, R. and Swindells, M. B. (2011). ‘LigPlot+: Multiple Ligand-Protein Interaction Diagrams for Drug Discovery’, *Journal of Chemical Information and Modelling*, 51 (10), pp. 2778-2786. *American Chemical Society Publications* [Online]. DOI: <https://doi.org/10.1021/ci200227u> (Accessed: 20 April 2022).

Li, J., Fu, A. and Zhang, L. (2019). ‘An Overview of Scoring Functions Used for Protein–Ligand Interactions in Molecular Docking’, *Interdisciplinary Sciences: Computational Life Sciences*, 11, pp. 320-328. *Springer Link* [Online]. DOI: <https://doi.org/10.1007/s12539-019-00327-w> (Accessed: 3 December 2021).

Lippert, T. and Rarey, M. (2009). ‘Fast Automated Placement of Polar Hydrogen Atoms in Protein-Ligand Complexes’, *Journal of Cheminformatics*, 1, 13. *Biomedcentral* [Online]. DOI: <https://doi.org/10.1186/1758-2946-1-13> (Accessed: 15 March 2022).

Morris, G. M., Goodsell, D. S., Pique, M. E., Lindstrom, W., Huey, R., Forli, S., Hart, W. E., Halliday, S., Belew, R. and Olson, A. J. (2014). ‘Automated Docking of Flexible Ligands to Flexible Receptors’, *User Guide: Autodock Version 4.2.6*. Available at: [https://autodock.scripps.edu/wpcontent/uploads/sites/56/2021/10/AutoDock4.2.6\\_UserGuide.pdf](https://autodock.scripps.edu/wpcontent/uploads/sites/56/2021/10/AutoDock4.2.6_UserGuide.pdf) (Accessed: 15 March 2022).

Morris, G. M., Huey, R. and Olson, A. J. (2008). ‘Using AutoDock for Ligand-Receptor Docking’, *Current Protocols in Bioinformatics*, Unit 8.14, pp. 1-40. *Wiley Interscience* [Online]. DOI: <https://doi.org/10.1002/0471250953.bi0814s24> (Accessed: 14 October 2021).

Morris, G. M., Huey, R., Lindstrom, W., Sanner, M. F., Belew, R. K., Goodsell, D. S. and Olson, A. J. (2009). ‘AutoDock4 and AutoDockTools4: Automated Docking with Selective Receptor Flexibility’, *Journal of Computational Chemistry*, 30 (16), pp. 2785-2791. *Wiley Online Library* [Online]. DOI: <https://doi.org/10.1002/jcc.21256> (Accessed: 15 November 2021).

Nadeau, R., Byvsheva, A. and Lavallée-Adam, M. (2021). ‘PIGNON: a Protein–Protein Interaction-Guided Functional Enrichment Analysis for Quantitative Proteomics’, *Biomedcentral Bioinformatics*, 302 (22). *Biomedcentral* [Online]. DOI: <https://doi.org/10.1186/s12859-021-04042-6> (Accessed: 20 February 2022).

Ördög, R. and Grolmusz, V. (2008). ‘Evaluating Genetic Algorithms in Protein-Ligand Docking’, In: Măndoiu I., Sunderraman R., Zelikovsky A. (eds) *Bioinformatics Research and Applications*, Lecture Notes in Computer Science, 4983. *Springer Link* [Online]. DOI: [https://doi.org/10.1007/978-3-540-79450-9\\_37](https://doi.org/10.1007/978-3-540-79450-9_37) (Accessed: 15 March 2022).

Pathania, S., Randhawa, V. and Kumar, M. (2019). ‘Identifying Potential Entry Inhibitors for Emerging Nipah Virus by Molecular Docking and Chemical-Protein Interaction Network’,



*Journal of Biomolecular Structure and Dynamics*, 38 (17), pp. 5108-5125. *Taylor and Francis Online* [Online]. DOI: <https://doi.org/10.1080/07391102.2019.1696705> (Accessed: 19 October 2021).

Rajput, A., Kumar, A., Megha, K., Thakur, A. and Kumar, M. (2021). 'DrugRepV: A Compendium of Repurposed Drugs and Chemicals Targeting Epidemic and Pandemic Viruses', *Briefings in Bioinformatics*, 22 (2), pp. 1076-1084. *Oxford Academic* [Online]. DOI: <https://doi.org/10.1093/bib/bbaa421> (Accessed: 10 November 2021).

Raveendran, A. V., Sadanandan, S., Thulaseedharan, N. K., Kumar, S., Pallivalappil, B. and Kumar, A. (2018). 'Nipah Virus Infection', *Journal of the Association of Physicians of India*, 66. *Association of Physicians India* [Online]. Available at: <https://www.japi.org/s2d49494/nipah-virus-infection> (Accessed: 10 November 2021).

Ren, J., He, Y., Chen, W., Chen, T., Wang, G., Wang, Z., Xu, Z., Luo, X., Zhu, W., Jiang, H., Shen, J. and Xu, Y. (2014). 'Thermodynamic and Structural Characterization of Halogen Bonding in Protein-Ligand Interactions: A Case Study of PDE5 and its Inhibitors', *Journal of Medicinal Chemistry*, 57 (8), pp. 3588-3593. *PubMed* [Online]. DOI: <https://doi.org/10.1021/jm5002315> (Accessed: 20 February 2022).

Ropón-Palacios, G., Chenet-Zuta, M. E., Olivos-Ramirez, G. E., Otazu, K., Acurio-Saavendra, J. and Camps, I. (2019). 'Potential Novel Inhibitors Against Emerging Zoonotic Pathogen Nipah Virus: A Virtual Screening and Molecular Dynamics Approach', *Journal of Biomolecular Structure and Dynamics*, 38 (11), pp. 3225-3234. *Taylor and Francis Online* [Online]. DOI: <https://doi.org/10.1080/07391102.2019.1655480> (Accessed: 23 October 2021).

Seeliger, D. and de Groot, B. L. (2010). 'Ligand Docking and Binding Site Analysis with PyMOL and Autodock/Vina', *Journal of Computer Aided Molecular Design*, 24, pp. 417-422. *Springer Link* [Online]. DOI: <https://doi.org/10.1007/s10822-010-9352-6> (Accessed: 15 November 2021).

Shivanika, C., Deepak, K. S., Venkataraghavan, R., Pawan, T., Sumitha, A. and Brindha, D. P. (2020). 'Molecular Docking, Validation, Dynamics Simulations, and Pharmacokinetic Prediction of Natural Compounds Against the SARS-CoV-2 Main-Protease', *Journal of Biomolecular Structure and Dynamics*, 40 (2), *Taylor and Francis Online* [Online]. DOI: <https://doi.org/10.1080/07391102.2020.1815584> (Accessed: 20 April 2022).

Simons, R. R. L., Gale, P., Horigan, V., Snary, E. and Breed, A. C. (2014). 'Potential for Introduction of Bat-Borne Zoonotic Viruses into the EU: A Review', *Molecular Diversity Preservation International Open Access Journals*, 6 (5), pp. 2084-2121. *Molecular Diversity Preservation International* [Online]. DOI: <https://doi.org/10.3390/v6052084> (Accessed: 2 December 2021).

Sun, B., Jia, L., Liang, B., Chen, Q. and Liu, D. (2018). 'Phylogeography, Transmission, and Viral Proteins of Nipah Virus', *Virologica Sinica*, 33, pp. 385-395. *Springer Link* [Online]. DOI: <https://doi.org/10.1007/s12250-018-0050-1> (Accessed: 4 November 2021).

Tripathi, A. and Bankaitis, V. A. (2017). 'Molecular Docking: From Lock and Key to Combination Lock', *Journal of Molecular Medicine and Clinical Applications*, 2 (1), *PubMed* [Online]. DOI: <https://doi.org/10.16966/2575-0305.106> (Accessed: 15 March 2022).

Wagner, J. R., Churas, C. P., Liu, S., Swift, R. V., Chiu, M., Shao, C., Feher, V. A., Burley, S. K., Gilson, M. K. and Amaro, R. E. (2019). 'Continuous Evaluation of Ligand Protein



Predictions: A Weekly Community Challenge for Drug Docking', *Structure*, 27 (8), pp. 1326-1335. *ScienceDirect* [Online]. DOI: <https://doi.org/10.1016/j.str.2019.05.012> (Accessed: 11 November 2021).

Wallace, A. C., Laskowski, R. A. and Thornton, J. M. (1995). 'LIGPLOT: A Program to Generate Schematic Diagrams of Protein-Ligand Interactions', *Protein Engineering, Design and Selection*, 8 (2), pp. 127-134. *Oxford Academic* [Online]. DOI: <https://doi.org/10.1093/protein/8.2.127> (Accessed: 15 November 2021).

Watkinson, R. E. and Lee, B. (2016). 'Nipah Virus Matrix Protein: Expert Hacker of Cellular Machines', *Federation of European Biochemical Societies: Letters*, 590 (15), pp. 2494-2511. *PubMed* [Online]. DOI: <https://doi.org/10.1002/1873-3468.12272> (Accessed: 7 October 2021).

World Health Organization. (2018). 'WHO Research and Development Blueprint 2018 Annual review of diseases prioritized under the Research and Development Blueprint'. *World Health Organization* [Online]. Available at: <http://www.who.int/csr/research-and-development/en/> (Accessed: 2 December 2021).

Xu, K., Broder, C. C. and Nikolov, D. B. (2012). 'Ephrin-B2 and Ephrin-B3 as Functional *Henipavirus* Receptors', *Seminars in Cell & Developmental Biology*, 23 (1), pp. 116-123. *ScienceDirect* [Online]. DOI: <https://doi.org/10.1016/j.semcdb.2011.12.005> (Accessed: 20 April 2022).

Yang, Y., Xu, Z., Zhang, Z., Yang, Z., Liu, Y., Wang, J., Cai, T., Li, S., Chen, K., Shi, J. and Zhu, W. (2015). 'Like-Charge Guanidinium Pairing between Ligand and Receptor: An Unusual Interaction for Drug Discovery and Design?', *The Journal of Physical Chemistry B*, 119 (36), pp. 11988-11997. *PubMed* [Online]. DOI: <https://doi.org/10.1021/acs.jpcc.5b04130> (Accessed: 20 February 2022).

Zhang, W., Bell, E. W., Yin, M. and Zhang, Y. (2020). 'Edock: Blind Protein-Ligand Docking by Replica-Exchange Monte Carlo Simulation', *Journal of Cheminformatics*, 12 (37). *BioMed Central* [Online]. DOI: <https://doi.org/10.1186/s13321-020-00440-9> (Accessed: 11 November 2021).

Zheng, L., Meng, J., Jiang, K., Lan, H., Wang, Z., Lin, M., Li, W., Guo, H., Wei, Y. and Mu, Y. (2022). 'Improving Protein-Ligand Docking and Screening Accuracies by Incorporating a Scoring Function Correction Term', *Briefing in Bioinformatics*, bbac051. *Oxford Academic* [Online]. DOI: <https://doi.org/10.1093/bib/bbac051> (Accessed: 20 April 2022).

## ACKNOWLEDGEMENTS

I would like to express my profound gratitude and admiration to my research supervisor, Ms. Heshani Mudalige, and co-supervisor, Mr. Ominda Perera. The BMS IT department is appreciated for facilitating IT assistance and I thank my family for the support they provided.